# Structural properties of carbon peapods under extreme conditions studied using in situ x-ray diffraction

M. Chorro, Stéphane Rols, Jean Cambedouzou, Laurent Alvarez, Robert Almairac, Jean-Louis Sauvajol, Jean-Louis Hodeau, L. Marques, M. Mezouar, H. Kataura

▶ **To cite this version:**

M. Chorro, Stéphane Rols, Jean Cambedouzou, Laurent Alvarez, Robert Almairac, et al.. Structural properties of carbon peapods under extreme conditions studied using in situ x-ray diffraction. Physical Review B: Condensed Matter and Materials Physics (1998-2015), 2006, 74 (20), pp.205425-1-5. 10.1103/PhysRevB.74.205425 . hal-00498754

**HAL Id: hal-00498754**
**https://hal.science/hal-00498754**

Submitted on 13 Dec 2019

**HAL** is a multi-disciplinary open access archive for the deposit and dissemination of scientific research documents, whether they are published or not. The documents may come from teaching and research institutions in France or abroad, or from public or private research centers.

L'archive ouverte pluridisciplinaire **HAL**, est destinée au dépôt et à la diffusion de documents scientifiques de niveau recherche, publiés ou non, émanant des établissements d'enseignement et de recherche français ou étrangers, des laboratoires publics ou privés.

# Structural properties of carbon peapods under extreme conditions studied using *in situ* x-ray diffraction

M. Chorro,* S. Rols,† J. Cambedouzou,* L. Alvarez, R. Almairac, and J.-L. Sauvajol
*Laboratoire des Colloïdes, Verres et Nanomatériaux (UMR CNRS 5587), Université Montpellier II, 34095 Montpellier Cedex 5, France*

J.-L. Hodeau
*Laboratoire de Cristallographie, CNRS, Boîte Postale 166 Cedex 09, 38000 Grenoble, France*

L. Marques
*Departamento de Física and CICECO, Universidade de Aveiro, 3800 Aveiro, Portugal*

M. Mezouar
*ESRF, Rue Jules Horowitz, Boîte Postale 220, 38043, Grenoble Cedex, France*

H. Kataura
*Nanotechnology Research Institute, National Institute of Advanced Industrial Science and Technology (AIST), Central 4, Higashi 1, Tsukuba, Ibaraki 305-8562, Japan*

(Received 11 September 2006; revised manuscript received 11 October 2006; published 21 November 2006)

Structural properties of carbon peapods, $C_{60}$, trapped into single-walled carbon nanotubes (SWNT), have been studied under high-pressure/high-temperature conditions (HPHT) by *in situ* x-ray diffraction. The $C_{60}$ chain structure together with the influence of the filling on the SWNT change under HPHT treatment is investigated. Synthesis of a one-dimensional polymer chain of $C_{60}$ inside the single-walled carbon nanotubes is evidenced. At 4 GPa, increasing the temperature up to 1023 °C leads to a progressive $C_{60}$ polymerization that is associated to a shortening of $C_{60}$-$C_{60}$ distance down to 8.7 Å. Back to ambient conditions, the $C_{60}$ chain remains polymerized, emphasizing the high stability of this material. In addition, our data strongly suggest a symmetry change of the two-dimensional bunde lattice under pressure.

DOI: 10.1103/PhysRevB.74.205425 PACS number(s): 61.46.Fg, 61.10.Nz, 61.48.+c

## I. INTRODUCTION

The discovery of peapods ($C_{60}$ encapsulated inside single-walled carbon nanotubes)[1,2] has opened new and fascinating possibilities to make building blocks for nanoengineering applications and many experimental and theoretical studies have recently been focused on those new hybrid all-carbon based nanostructures. In particular, the synthesis of a one-dimensional polymer crystal of $C_{60}$ along the nanotube axis at a pressure ~10 GPa has been recently evidenced by an *in situ* x-ray diffraction (XRD) experiment.[3] This work is an additional evidence that various polymeric phases of $C_{60}$ may coexist inside the hollow core of the nanotubes under certain conditions and corroborates previous experimental works: Pichler *et al.* used Raman spectroscopy on potassium doped peapods to reveal the formation of a metallic polymer state[4] unstable in air; Cambedouzou *et al.* showed that a part of the $C_{60}$ inserted inside the SWNT stand as $n$-mer chains (with $n=2,3,\ldots$) using inelastic neutron scattering at ambient pressure and temperature.[5] Other investigations using Raman and transmission electron microscopy (TEM) have also revealed the transformation of the peapods into double-walled carbon nanotubes (DWNT) from the fusion of the $C_{60}$ at a temperature of 1020 °C.[6] Therefore the phase diagram of the peapods is rich, ranging from the monomer to the one-dimensional (1D)-polymer phase and to the complete transformation into DWNT. This characteristic is inherent to the $C_{60}$ molecule for which a whole set of dimer, 1D, 2D, and even 3D polymer phases has already been studied by many authors as a function of pressure and temperature. In this paper, we report an *in situ* x-ray diffraction investigation under high pressure/high temperature (HPHT) conditions. This study sheds light on the evolution of the 2D-lattice of the bundle as a function of pressure, and highlights the role of temperature on the pressure of polymerization.

## II. SAMPLE DESCRIPTION AND EXPERIMENTAL SETUP

The peapod sample was prepared using a synthesis method reported elsewhere[7] and was characterized by several techniques: Raman, TEM, and XRD.[7,8] The peapods sample is made from buckypapers. Before the HTHP cycle, small pieces of this paper were cut and were characterized in our laboratory using a powder diffractometer. After the HPHT cycle, the sample was measured again in our laboratory. The XRD *in situ* experiment under HPHT conditions was carried out on the ID30 beamline at the ESRF, using a wavelength of 0.619 926 Å. A Paris-Edimbourg pressure cell was used to reach a pressure of 4 GPa. In order to keep the pressure as hydrostatic as possible, a boron-nitride (BN) environment was introduced into the pressure cell around the small pieces of buckypaper. During the experiment, several points of temperature ($T$) and pressure ($P$) were considered. The XRD patterns were successively recorded for each of the following $[T,P]$ points: [Room temperature, Room pressure] ([RT,RP]), [RT, 1 GPa], [RT, 2 GPa], [RT, 3 GPa], [RT,

 ©2006 The American Physical Society

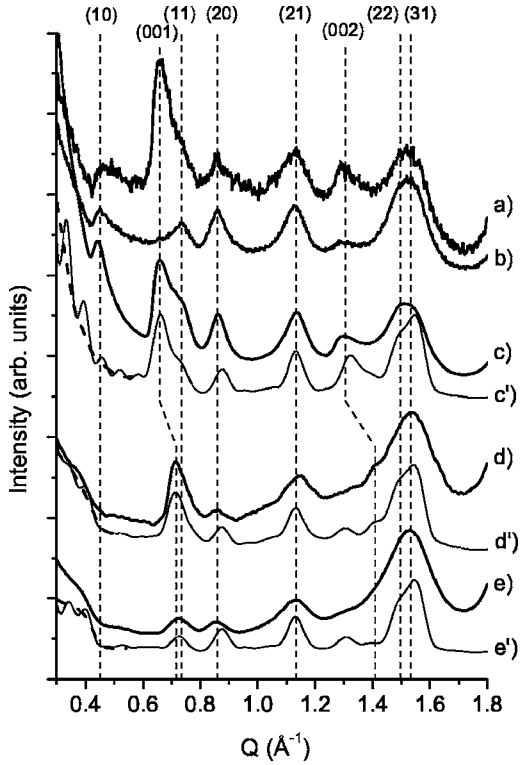


FIG. 1. X-ray diffraction patterns of the peapods sample at room pressure and room temperature: (a) paper parallel to the diffraction plane (DP), (b) paper perpendicular to the DP, (c) Synchrotron XRD diagram, (c′) numerical diagram accounting for a 2D orientation of the tubes axis in the plane of the paper (see text), (d) and (e) diffraction patterns measured on the sample (cylinder) after the (HPHT) cycle for two different orientations (see text), and (d′) and (e′) corresponding calculations of the diagram.

4 GPa], [340 °C, 4 Gpa], [560 °C, 4 GPa], [770 °C, 4 GPa], [1020 °C, 4 GPa], [550 °C, 4 GPa], [RT, 4 GPa], and finally [RT, RP].

## III. THE NUMERICAL MODEL

All the experimental diffraction patterns are compared to diagrams calculated with a convenient model.[8] In this model, first we calculate the scattering amplitude $A(\mathbf{Q})$ as the Fourier transform of the bundle of peapods (where $\mathbf{Q}$ is the wave-vector transfer) and second we calculate the intensity function $I(Q)=\langle p(\mathbf{Q})\|A(\mathbf{Q})\|^2\rangle$ where $p(\mathbf{Q})$ describes the statistic of our sample and where the average is made over $\mathbf{Q}$ orientations and eventually over sample structural parameter. As an example $p(\mathbf{Q})$ can take into account a diameter distribution of the tubes or an orientational effect in the sample. Finite size effects and form factors of the tube and of the $C_{60}$ are automatically taken into account using this procedure. A number of 15 $C_{60}$ molecules per chain was found to be enough to reproduce the diffraction patterns. However, these short chains produce undesirable small oscillations in the calculated curves at small $Q$ [below the (10) position—see Fig. 1]. This region is very difficult to reproduce by using such models for which no impurities are introduced into the numerical samples, and for which a single cylindrical shape is kept for the bundles. As is very well-known in the nanotube community, the real samples contain a non-negligible amount of carboneous nanoparticles the response of which is mainly important at low $Q$ values. Moreover, as observed from TEM images, the general shape of the bundle is multiple and variable. This results in the smoothing out of the low $Q$ features and only a small angle background in the experimental diagrams is observed. Therefore no effort was made to reproduce this part of the experimental diagram. For comparison we can replace the oscillating curves by the mean value in this $Q$ region as shown by the dashed lines in Fig. 1.

## IV. SAMPLE CHARACTERIZATION BEFORE AND AFTER THE HPHT CYCLE

In Fig. 1 we present diffraction patterns obtained at room temperature and room pressure. The two experimental diagrams (a) and (b) were measured on the pristine sample before the HPHT cycle in our laboratory, for two orientations of the paper with respect to the diffraction plane: (a) the paper is parallel to the diffraction plane and (b) it is perpendicular. One observes a strong difference on the (001) and (002) lines concerning the $C_{60}$ chain ordering. This is characteristic of an orientation of the tubes which is an effect already observed and discussed[9–11] for pristine nanotubes and peapods in the form of buckypapers. However, this orientation is observed to be particularly strong in our paper [see the (a) and (b) diagrams in Fig. 1] and the strong intensity of the (001) line in the diagram (a) suggests that the tubes axes are lying in the plane of the paper at RTRP with a very weak out of plane mosaic angle. Applying a fitting procedure, we have obtained a very good agreement in between the RTRP experimental patterns of the papers and diagrams calculated for a perfect orientation of the tubes axes in the plane of the paper and with bundles of 37 tubes each having a 6.8 Å radius (16.8 Å lattice parameter) and filled at their maximum with chains of 15 $C_{60}$ separated by a center-to-center distance of 9.8 Å. As the details of the calculations are published elsewhere[8] the calculated curves are not shown here.

Curve (c) is the XRD pattern measured on the synchrotron beamline (first point [RTRP] of the HPHT cycle). Although the pressure is supposed to be 0 GPa, it is not really the case (P slightly departs from 0 GPa as soon as the pressure cell is closed) and an orientational effect is clearly observed on the diagram as it strongly resembles curve (a) which suggests that the tubes present a preferential orientation inside the pressure cell. Curve (c′) (thin line) has been calculated for the case of an orientation identical to that of curve (a). The excellent agreement (except the very low $Q$ range—see previous section) gives confidence on the validity of the model parameters. The pressure induced orientation has been confirmed by the measurements performed in our laboratory after the HPHT cycle. The sample extracted from the cell was found to be transformed into a very compact and hard black cylinder with 1 mm diameter and 2.5 mm length. The diffraction patterns (d) and (e) measured for two differ-

ent orientations of the cylinder with respect to the diffraction plane are to be compared to curves (a) and (b). As in the case of the pristine sample a clear orientational effect is observed. By taking account of a 1D orientation of the tubes along the black cylinder axis (due to the cylindrical geometry of the actual sample) with a mosaic angle of 95°, a very good agreement is found in between our calculations [thin line curves (d′) and (e′)] and the data. This orientation has two consequences: (i) it is important to take it into account for model calculations and (ii) it is very favorable for the determination of the inter $C_{60}$ distance as it enhances the intensity of the (00l) reflections. The structural parameters of the bundles and of the tubes are kept unchanged but the inter $C_{60}$ distance is reduced to 9.1 Å. This implies that the nature of the bonds in between the $C_{60}$ has been changed by the HPHT treatment. The 9.1 Å inter $C_{60}$ distance which is much shorter than the initial one suggests that the $C_{60}$ molecules are linked by the so-called [2+2] cycloaddition for which $C_{60}$ are covalently bonded. No major modification of the structure of the bundles are observed. However, we point out that the intensity of the (10) line from the bundles is much reduced in the experimental diagrams after cycle compared to the initial diagrams. This might indicate a probable destruction of the tubes—or the parts of them—that were not filled up with $C_{60}$, in agreement with previous work.[3,12] In that case, the presence of the $C_{60}$ inside the nanotubes reinforces the nanotubes.

## V. PRESSURE DEPENDENCE OF THE DIFFRACTION DIAGRAMS

Figure 2(d) shows the experimental XRD patterns of the peapod sample as a function of the pressure applied from [RT, RP] up to [RT, 4 GPa] measured at the synchrotron beamline. When pressure is applied, one can observe that all the diffraction lines originating from the bundles packing are very much affected: they all broaden and shift to higher $Q$ values, however, this shift is nonhomothetic and the broadening is very dependent on the line under study, e.g., on the value of the $(hkl)$ indices of the Bragg reflection. As an illustration, let us focus our discussion on the (11), (20), and (21) features located at 0.74, 0.86, and 1.13 $Å^{-1}$, respectively (at $P=0$ GPa). The (11) line is very sensitive to pressure and shifts quickly to higher $Q$ values. Its intensity is strongly reduced as its position matches the second zero of the Bessel function (around 0.8 $Å^{-1}$) representing the form factor of a tube and which is characteristic of their diameter. The same behavior is observed for the (21) line and its width broadens quickly with pressure. By contrast, the position width and intensity of the (20) reflection is much less pressure dependent. In particular, its position shifts only slightly from 0.86 to 0.88 $Å^{-1}$. This effect has also been observed by Kawasaki *et al.*[3] in a larger pressure range. In view of extracting the different structural parameters (inter $C_{60}$ distance, lattice parameter, and van der Waals distance between tubes) a different scenario concerning a structural modification of the bundle has been considered in the calculations. All models preserving the hexagonal symmetry of the bundle like the hard cylinders model or a model accounting for a complete

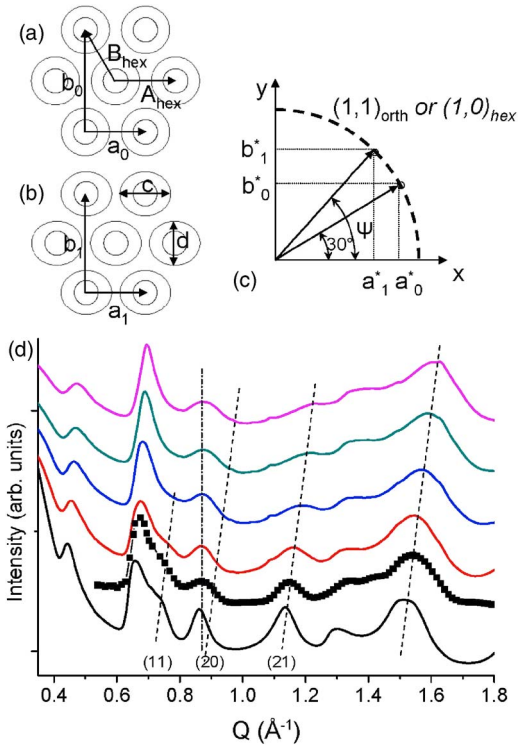


FIG. 2. (Color online) (a) and (b) Deformation of the bundle lattice accounting for an ovalization of the nanotubes; (c) example of transformation of the reciprocal lattice of the bundle to keep the length of the $Q_{(11)_{ortho}}$ reflection unchanged; and (d) full lines: Synchrotron diffraction patterns of the peapods samples at room temperatures and from bottom to top: RP, 1 GPa, 2 GPa, 3 GPa, and 4 GPa. The diagrams were normalized to their intensity integrated from 0.2 to 1.9 $Å^{-1}$. The dashed lines are parallel lines to guide the eye. The dashed-dotted line is a vertical line used to highlight the weak dependence of the (20) reflection. Closed squares: numerical pattern calculated for a transformation of the bundle lattice characterized by a value of 0.86 for the coefficient of flatness and a value of $\psi=31.8°$ (see text).

facetization of the tubes[13] have been tried. They all fail to reproduce correctly the data. Consequently we must consider a different hypothesis, one of the simplest being that the hexagonal symmetry is no longer preserved. This is strongly suggested by the observations, i.e., broadening and sensitivity of the $(hk)$ components and weak sensitivity of the $(h0)$ components. The simplest symmetry change to be considered is a hexagonal-to-orthorhombic transition under pressure which can be understood by taking into account the multiple unit cell $(a,b)$ as represented in Figs. 2(a) and 2(b). In this rectangular centered cell, we suppose that a deformation of the lattice occurs via an ovalization of the nanotubes leading to a shortening of the lattice parameter $b$ concomitant to an increase of the lattice parameter $a$. The (10) line in the hexagonal system is indexed $(11)_{orth}$ in the rectangular (orthorhombic) system. In our model we assume that the length of the $\mathbf{Q}(11)_{orth}$ vector remains unchanged under the deformation. Therefore all the deformations of the bundle lattice

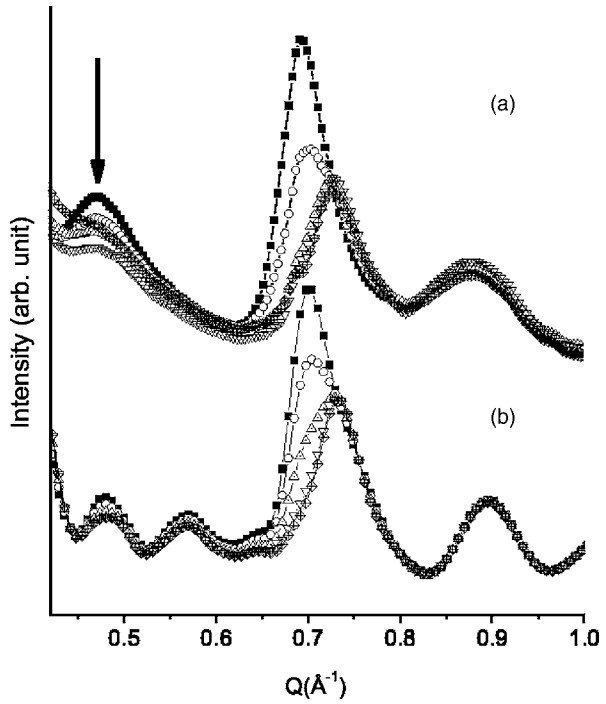


FIG. 3. (a) X-ray diffraction patterns of the peapods samples at 4 GPa and at room temperature (closed squares), 340 °C (open circles), 560 °C (triangles up), 770 °C (triangles down), and 1020 °C (diamonds). (b) Numerical diagram obtained by accounting for a mixture of monomer and polymer phases: 100% monomer (closed squares), 70% monomer (open circles), 40% monomer (triangles up), 20% monomer (triangles down), and 15% monomer (diamonds).

keeping the $(11)_{orth}$ diffraction line unchanged in position can be constructed by putting the extremity of the $\mathbf{Q}(11)_{orth}$ vector on a circle as shown in Fig. 2(c). A peculiar transformation is characterized by the angle $\psi$ and by the coefficient of flatness $\epsilon=d/c$ where $c$ and $d$ are the long and short axis of the oval section of the nanotubes, respectively. As an example, we compare in Fig. 3(d) the diffraction diagram calculated for an ovalization characterized by a value $\epsilon=0.86$ and assuming a lattice deformation characterized by the angle $\psi=31.8°$. In contrast with the hexagonal models a very good agreement with the experimental diagram [RT, 1 GPa] is now obtained. In this calculation we account for a contraction of the fullerene radius from 3.5 to 3.25 Å. A 1D $C_{60}$ chain lattice parameter of 9.45 Å is also incorporated into the calculations.

As for the center-to-center $C_{60}$ distance, our calculations indicate that it varies from 9.8 Å at RTRP down to 9.1 Å at 4 GPa leading to a C-C distance of 2.1 Å if the shape of the $C_{60}$ is assumed to be spherical.

We would like to emphasize that when the symmetry changes from hexagonal to orthorhombic, the six $(10)_{hexa}$ reflections are replaced by four $(11)_{orth}$ reflections and two new $(02)_{orth}$ reflections. However, the distance between these $(11)_{orth}$ and $(02)_{orth}$ reflections is only 0.02 Å$^{-1}$ for a value of $\psi=31.8°$, which is too small in regard to the linewidth of the reflections. Therefore such splitting cannot be observed in the diffraction patterns. It is of some importance to remark also that this type of calculation (based on a Fourier transform of the bundle) takes automatically into account these two kinds of reflection. Finally, we note that such a pressure induced ovalization of a SWNT has been previously considered for the interpretation of diffraction data.[14]

## VI. TEMPERATURE DEPENDENCE OF THE DIFFRACTION DIAGRAMS AT 4 GPa

From the point at [RT, 4 GPa], the temperature was increased gradually up to 1020 °C. Figure 3(a) shows the diffraction diagrams in the [0.45, 0.85 Å$^{-1}$] range to highlight the evolution of the diffraction lines from the 1D chain. One clearly observes a progressive upshift of the (001) line with increasing temperature up to a $Q$ value close to 0.73 Å$^{-1}$. Such a value corresponds to a lattice parameter of about 8.7 Å which would lead to an inter-$C_{60}$ bond of 1.7 Å assuming that the $C_{60}$ shape is not deformed by the pressure and temperature treatment. This value is in very good agreement with the experimental (see Ref. 15 for an example) and theoretical[16] values of the C–C bonds in the 1D polymer orthorhombic phase of $C_{60}$ obtained by HPHT treatment of $C_{60}$ in its monomer cubic phase. Therefore we interpret the shortening of the inter-$C_{60}$ distance as a polymerization of the $C_{60}$ chains inside the nanotubes as temperature is being increased at 4 GPa. To verify this hypothesis we calculated the diffraction diagrams for a mixture of monomer and polymer phases of the peapods. The results are shown in Fig. 3(b). We observe a good agreement in between the experimental and the numerical diagram by considering a progressive polymerization of the peapods with temperature. The lowering of the (001) line from the chain is due to the modulation of its intensity by the $C_{60}$ form factor which is decreasing with $Q$ in this $Q$ region. In the low $Q$ part of the diagram we observe a progressive disappearance of the signal at the (10) position [see the arrow in Fig. 3(a)]. This leads to the final shape of the diagram in that range as discussed in the first part of this paper. This might indicate the destruction of the nanotubes or the part of them that are not filled with $C_{60}$.[3,12]

## VII. DISCUSSION AND CONCLUSION

In conclusion, we have shown that polymerization of the $C_{60}$ inside the nanotubes is achievable by increasing the temperature at a pressure of 4 GPa. This pressure is noticeably smaller than the one previously reported by Kawasaki and coworkers.[3] The chemical reaction is therefore thermically activated. Actually, bringing the $C_{60}$ closer to each other might induce a progressive orientation of the $C_{60}$ in such a way that polymerization becomes possible. The role of temperature is to increase the probability per unit of time that this orientation happens. As a consequence, polymerization of the peapods sample is expected to occur even at lower

pressure as soon as temperature is increased. Further experiments are scheduled to explore more precisely the $P$ and $T$ phase diagram of the peculiar nanomolecular device. We have also highlighted the ovalization of the nanotubes under pressure, even when filled with $C_{60}$. It is very interesting to observe that the confinement of the $C_{60}$ inside the nanotubes has the effect of protecting the nanotubes from destruction.

## ACKNOWLEDGMENT

One of us (L. M.) thanks F. C. T. (Lisbon, Portugal) for financial support.

*Present address: Laboratoire de Physique du Solide, Orsay Cedex, 91405, France.

†Also at Institut Laue Langevin, 38042 Grenoble, France.

[1] B. W. Smith, M. Monthioux, and D. E. Luzzi, Nature (London) **396**, 323 (1998).

[2] B. W. Smith and D. E. Luzzi, Chem. Phys. Lett. **321**, 169 (2000).

[3] S. Kawasaki, T. Hara, T. Yokomae, F. Okino, H. Touhara, H. Kataura, T. Watanuki, and Y. Ohishi, Chem. Phys. Lett. **418**, 260 (2006).

[4] T. Pichler, H. Kuzmany, H. Kataura, and Y. Achiba, Phys. Rev. Lett. **87**, 267401 (2001).

[5] J. Cambedouzou, S. Rols, R. Almairac, J.-L. Sauvajol, H. Kataura, and H. Schober, Phys. Rev. B **71**, 041403(R) (2005).

[6] S. Bandow, M. Takizawa, K. Hirahara, M. Yudasaka, and S. Iijima, Chem. Phys. Lett. **337**, 48 (2001).

[7] H. Kataura, Y. Maniwa, T. Kodama, K. Kikuchi, K. Hirahara, K. Suenaga, S. Iijima, S. Suzuki, Y. Achiba, and W. Krätschmer, Synth. Met. **121**, 1195 (2001).

[8] J. Cambedouzou, V. Pichot, S. Rols, P. Launois, P. Petit, R. Klement, H. Kataura, and R. Almairac, Eur. Phys. J. B **42**, 31 (2004).

[9] N. Bendiab, R. Almairac, J.-L. Sauvajol, S. Rols, and E. Elkaim, J. Appl. Phys. **93**, 1769 (2003).

[10] R. Almairac, J. Cambedouzou, S. Rols, and J. L. Sauvajol, Eur. Phys. J. B **49**, 147 (2006).

[11] W. Zhou, K. I. Winey, J. E. Fischer, T. V. Sreekumar, S. Kumar, and H. Kataura, Appl. Phys. Lett. **84**, 2172 (2004).

[12] S. Kawasaki, Y. Matsuoka, T. Yokomae, Y. Nojima, F. Okino, H. Touhara, and H. Kataura, Carbon **43**, 37 (2005).

[13] S. Rols, I. N. Gontcharenko, R. Almairac, J. L. Sauvajol, and I. Mirebeau, Phys. Rev. B **64**, 153401 (2002).

[14] S. Karmakar, S. M. Sharma, and A. K. Sood, Nucl. Instrum. Methods Phys. Res. B **238**, 281 (2005).

[15] M. Nuñez-Regueiro, L. Marques, J.-L. Hodeau, O. Bethoux, and M. Perroux, Phys. Rev. Lett. **74**, 278 (1995).

[16] G. B. Adams, J. B. Page, O. F. Sankey, and M. O'Keeffe, Phys. Rev. B **50**, 17471 (1994).